Developmental Cell, Vol. 5, 487–498, September, 2003, Copyright ©2003 by Cell Press

The COPI Complex Functions in Nuclear Envelope Breakdown and Is Recruited by the Nucleoporin Nup153

Jin Liu, Amy J. Prunuske, Ammon M. Fager, and Katharine S. Ullman*
Department of Oncological Sciences
Huntsman Cancer Institute
2000 Circle of Hope
University of Utah
Salt Lake City, Utah 84112

Summary

Nuclear envelope breakdown is a critical step in the cell cycle of higher eukaryotes. Although integral membrane proteins associated with the nuclear membrane have been observed to disperse into the endoplasmic reticulum at mitosis, the mechanisms involved in this reorganization remain to be fully elucidated. Here, using *Xenopus* extracts, we report a role for the COPI coatomer complex in nuclear envelope breakdown, implicating vesiculation as an important step. We have found that a nuclear pore protein, Nup153, plays a critical role in directing COPI to the nuclear membrane at mitosis and that this event provides feedback to other aspects of nuclear disassembly. These results provide insight into how key steps in nuclear division are orchestrated.

Introduction

For much of the cell cycle, eukaryotic genomic DNA is enclosed by two membrane bilayers termed the nuclear envelope. Thousands of macromolecular nuclear pore complexes are present in this nuclear envelope and serve as conduits for traffic between the nucleus and cytoplasm (Vasu and Forbes, 2001; Suntharalingam and Wente, 2003). Despite the continuity at each nuclear pore between the inner and outer nuclear membranes, a unique profile of proteins are anchored in the inner nuclear membrane through interactions with proteins located at the peripheral nuclear lamina and chromatin (Burke and Ellenberg, 2002). In metazoan cells, the nuclear envelope becomes reorganized at mitosis, and ultimately its disassembly is key to accurate inheritance of both genomic DNA and nuclear envelope components.

Events proposed to be important to the disintegration of the nuclear envelope include: changes in nuclear pore configuration (Lenart et al., 2003; Terasaki et al., 2001); creation of a tear in the nuclear envelope due to microtubule-dependent tension exerted on the nuclear envelope (Beaudouin et al., 2002; Salina et al., 2002); and an increase in lateral mobility of integral membrane proteins allowing equilibration between the nuclear envelope and the endoplasmic reticulum and resulting in the loss of distinction between these membrane populations (Ellenberg et al., 1997; Yang et al., 1997). Observations that there are specific subtypes of vesicle populations necessary for nuclear envelope formation in vitro (Buendia and Courvalin, 1997; Drummond et al., 1999; Ewald et al., 1997; Sasagawa et al., 1999; Vigers and Lohka, 1991) support the idea that formation of specialized vesicles occurs at mitosis. An alternative interpretation of this data is that specialized microdomains within the mitotic endoplasmic reticulum are the source of specialized vesicles, which are generated only when this membrane network is fragmented during biochemical fractionation (Collas and Courvalin, 2000; Ellenberg et al., 1997). Indeed, recent models have discounted vesiculation as a step of nuclear envelope breakdown (Aitchison and Rout, 2002; Burke and Ellenberg, 2002; Collas and Courvalin, 2000; Gonczy, 2002; Lenart and Ellenberg, 2003).

Nuclear pore proteins (nucleoporins or Nups), situated in intimate connection with the nuclear membrane, are uniquely positioned to help execute nuclear envelope breakdown. However, outside the context of facilitating nucleocytoplasmic trafficking of cell cycle factors, a role for nucleoporins in nuclear envelope disassembly has not been reported. Nup153 is dynamically associated with the pore (Daigle et al., 2001) with a steady-state localization on the nuclear face of the pore and regions exposed on the cytoplasmic side as well (Fahrenkrog et al., 2002; Nakielny et al., 1999; Pante et al., 1994; Sukegawa and Blobel, 1993; Walther et al., 2001). Here, we explored the function of Nup153 in nuclear envelope disassembly and discovered a critical role for this pore protein in nuclear envelope breakdown. To better understand this role, we identified proteins that interact with the central region of Nup153 and surprisingly found an association between Nup153 and the COPI complex. This coatomer complex has been previously characterized in the context of vesicle budding during trafficking both within the Golgi and between Golgi and ER (Nickel et al., 2002). We find that perturbing the function of the COPI complex dramatically impairs nuclear envelope disassembly. These results lend insight into key players at this important stage of the cell cycle. Moreover, our data link the machinery of vesicular trafficking to nuclear envelope breakdown, indicating a greater complexity to this process than currently appreciated, but giving new clues about the mechanisms that are involved.

Results

The Nucleoporin Nup153 Plays a Critical Role in Nuclear Envelope Breakdown

To investigate whether Nup153 participates in nuclear envelope breakdown, we examined whether recombinant fragments of Nup153 exert dominant-negative effects on this process in vitro. We used cell-free extracts derived from *Xenopus* eggs to form synthetic nuclei around sperm chromatin. This system offers the advantage of biochemical manipulation, while being well established to robustly recapitulate both nuclear assembly as well as nuclear disassembly in response to mitotic signals (Murray et al., 1989). Cycloheximide was included to prevent synthesis of cyclin, thereby arresting

*Correspondence: katharine.ullman@hci.utah.edu

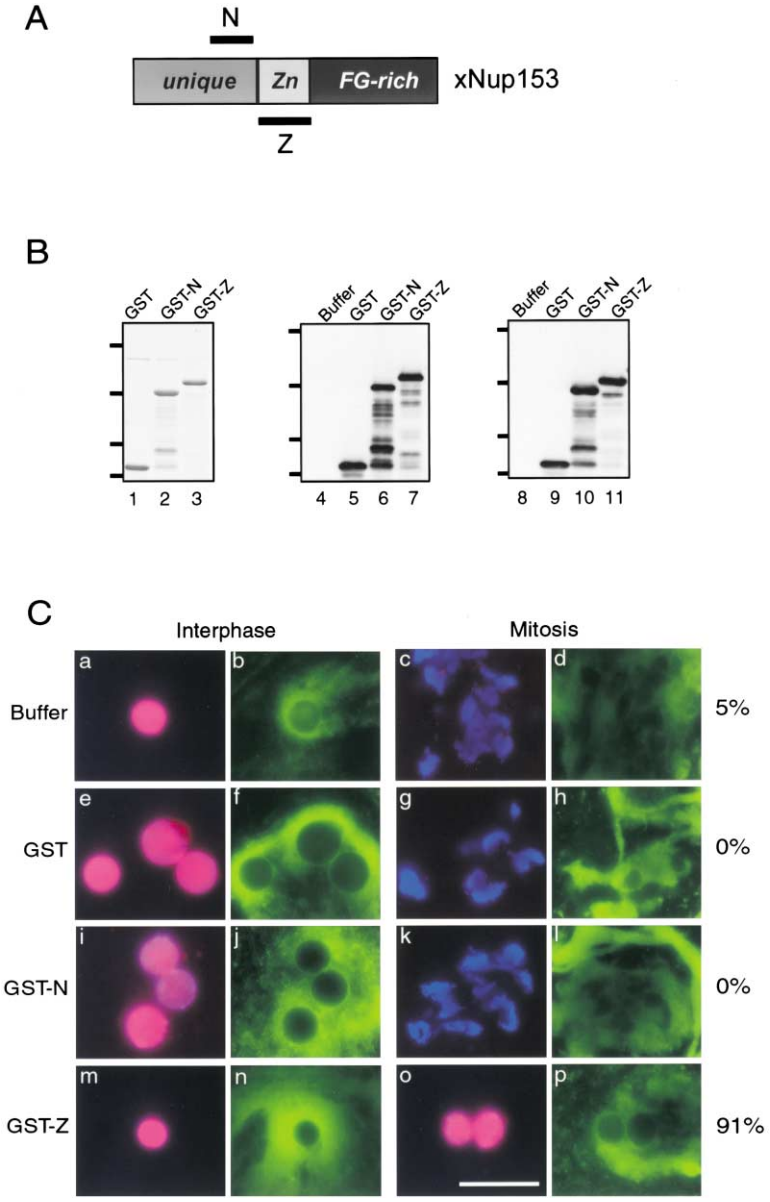

Figure 1. A Specific Domain of Nup153 Exerts a Dominant-Negative Effect on Nuclear Envelope Breakdown

(A) Schematic diagram of *Xenopus* Nup153. "N" and "Z" indicate Nup153-N (amino acids 436–655) and Nup153-Z (amino acids 655–926) fragments used in this study.

(B) Coomassie blue staining of purified recombinant proteins GST, GST-N, and GST-Z (lanes 1–3). Immunoblot of recombinant proteins before (lanes 4–7) and after (lanes 8–11) nuclei assembly/disassembly assay. Proteins were detected with antibodies directed against GST. Molecular weight markers indicated correspond to 93, 49, 35, and 29 kDa.

(C) Buffer (ELB) or recombinant proteins (3 μg) were added 15 min prior to the beginning of the assembly/disassembly assay. The interphase sample was taken after 90 min of assembly, immediately prior to cyclin addition. The mitotic sample was taken 75 min after cyclin addition. DNA (Hoechst 33258 stain) is shown in blue and merged with the signal for NLS import substrate, shown in red (panels a, c, e, g, i, k, m, and o). Membrane staining is shown in panels b, d, f, h, j, l, n, and p. Numbers to the right of the panel indicate the percentage of intact nuclei at the 75 min post-cyclin time point. The bar in panel o indicates 50 μm.

these extracts in interphase. After nuclei were assembled, a recombinant form of stabilized cyclin B was added to initiate mitotic events. As expected, 20–40 min after addition of cyclin, the nuclei synchronously exhibited hallmark features of mitosis, including chromatin condensation and, after 75 min, the disappearance of a continuous nuclear membrane (Figure 1C, panels c and d). Detection of import cargo provided the clearest visualization of whether a nuclear envelope was intact. When a protein fragment derived from the unique N-terminal domain of Nup153 (GST-N; Figures 1A and 1B, lanes 2 and 6) was present, nuclear envelope breakdown occurred without any marked alterations (Figure 1C, panels k and l). A control GST fusion protein (Figure 1B, lanes 1 and 5) likewise had no effect (Figure 1C, panels g and h). However, when a fragment encompassing the central zinc finger domain of Nup153 (GST-Z; Figures 1A and 1B, lanes 3 and 7) was included, a striking inhibition of nuclear envelope breakdown was apparent (91% of nuclei remaining). Membrane-staining rims around the DNA, typical of the nuclear envelope, were observed in the presence of zinc finger even after cyclin addition (Figure 1C, panel p). In addition, nuclear import cargo was still concentrated in nuclei under mitotic conditions, confirming both the presence and integrity of the nuclear envelope (Figure 1C, panel o). The effect of the Nup153 zinc finger was not due to selective stability of this fragment, as equivalent levels of recombinant protein were detected in each reaction by immunoblot following the last time point (Figure 1B, lanes 9–11). It is noteworthy that nuclear assembly and NLS-mediated import proceeded in the presence of the zinc finger fragment, although there was a reduction in nuclear size (Figure 1C, panels m–p).

To be certain that the block imposed by this fragment was due to interference with a function attributable to

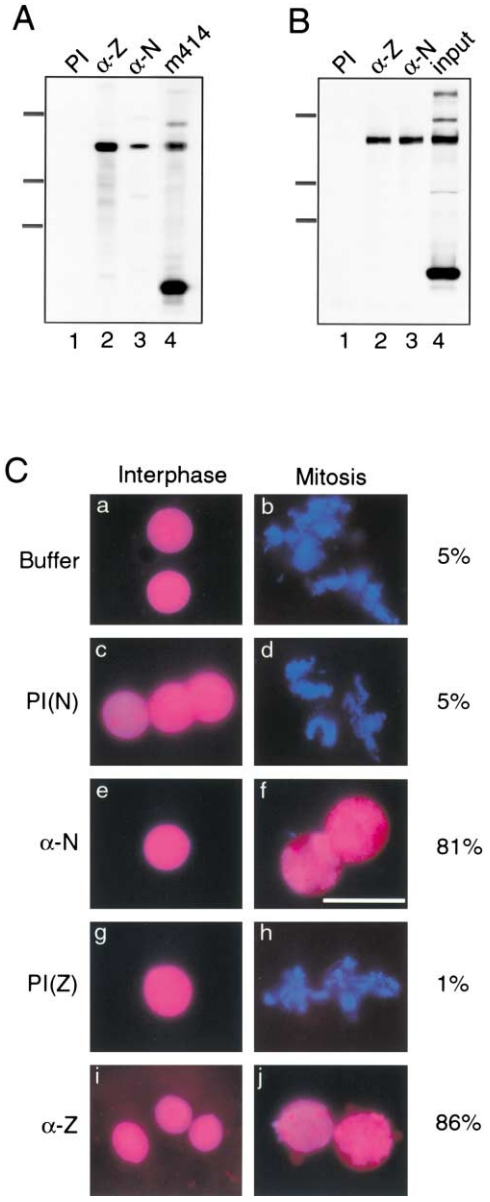

Figure 2. Antibodies Specific to Nup153 Interfere with Nuclear Envelope Breakdown

(A) Immunoblot of fractionated egg extract probed with preimmune antibody (lane 1), antibody against Nup153-Z (lane 2), antibody against Nup153-N (lane 3), and mAb414 (lane 4). mAb414 reactivity confirms the presence of Nup358, Nup214, Nup153, and Nup62. For both (A) and (B), molecular weight markers indicated are 198, 115, and 93 kDa.

(B) Immunoprecipitation of egg extract with preimmune (lane 1), anti-Nup153-Z (lane 2), and anti-Nup153-N (lane 3). Lane 4 was loaded with the equivalent of ~75% input. The blot was probed with mAb414.

(C) Preimmune (PI) or specific antibodies (2.5 μg) or buffer (ELB) was added 15 min prior to the beginning of the assembly/disassembly assay. Samples were processed as described in Figure 1. Nuclear import cargo and DNA are shown; the bar in panel f indicates 50 μm.

Nup153, we used antibodies that specifically recognize Nup153, as assessed by both immunoblot analysis (Figure 2A, lanes 2 and 3) and immunoprecipitation (Figure 2B, lanes 2 and 3). When these antibodies were included in the nuclear disassembly assay, they too prevented the normal progression of events: the nuclear membrane stayed largely intact (81%–86% nuclei remaining at the mitotic time point), as indicated by the accumulation of import cargo (Figure 2C, panels f and j) and membrane staining (data not shown). Of note, nuclear import mediated by a classical NLS took place as usual in the presence of these antibodies (Figure 2C, panels e and i), indicating that there was no impediment to this particular pathway or to general movement through the nuclear pore complex, consistent with previous studies (Ullman et al., 1999). Although we noted a difference in their potency, these two antibodies raised against different Nup153 domains interfered similarly with nuclear envelope breakdown, whereas antibodies purified from preimmune sera had no effect on nuclear envelope breakdown (Figure 2C, panels d and h).

Nup153 Associates with Members of the COPI Coatomer Complex

Although various proteins are known to associate with Nup153, none provides a clear link to nuclear disassembly (Hang and Dasso, 2002; Moroianu et al., 1997; Nakielny et al., 1999; Shah and Forbes, 1998; Shah et al., 1998; Smythe et al., 2000; Vasu et al., 2001; Zhang et al., 2002). To search for partners that would lend insight into how the zinc finger domain exerts its dominant-negative effect, recombinant zinc finger protein was immobilized on sepharose beads and incubated in *Xenopus* egg extract. After several rounds of washes, proteins that remained associated were analyzed and compared to a parallel preparation using immobilized GST (Figure 3A, lanes 2 and 3). Mass spectrometry analysis revealed that three members of the COPI coatomer complex (β, β′, and α) specifically associated with the Nup153 zinc finger region (Figure 3B). Other members of this complex would not have been detected, as we had concentrated our efforts on proteins larger than 55 kDa due to the interference of the fusion protein in the analysis of smaller proteins. Identification of COPI components in association with the zinc finger domain of Nup153 was confirmed by immunoblot analysis of similarly prepared samples (Figure 3C). Two bands were observed when the antibody against human β-COP was used to detect *Xenopus* proteins (Figure 3C, lane 3), and only the upper band appears to associate with the zinc finger fragment. The nature of this doublet is not yet understood. Antibodies raised against the analogous region of *Xenopus* β-COP detect only one major product (see below; Figure 4).

To determine the significance of the interaction between the coatomer proteins and this nucleoporin domain, we evaluated whether the COPI complex has a role in nuclear disassembly. Antibodies that immunoprecipitate human COPI components did not work well in immunoprecipitations from egg extract, indicating that their recognition of native *Xenopus* coatomer proteins was inefficient (data not shown). We therefore raised an antibody using a peptide derived from the sequence of *Xenopus* β-coatomer. These antibodies detect β-coatomer among a complex mixture of proteins on an immunoblot (Figure 4A, lane 2) and recognize native protein in immunoprecipitations (Figure 4B, lane 2). Addition

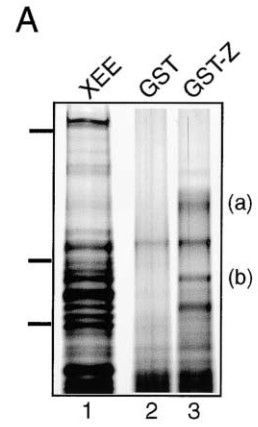

B

(a)

Peptide 1		HVLEGHDR
α-COP	199	HVLEGHDR 206
Peptide 2		DVAVMQLR
α-COP	351	DVAVMQLR 358
Peptide 3		ASNLENSTYDLYTIPK
α-COP	383	ASNLENSTYDLYTIPK 398
Peptide 4		SSGLTAVWVAR
α-COP	413	SSGLTAVWVAR 423
Peptide 5		TLDLPIYLTR
α-COP	563	TLDLPIYVTR 572
Peptide 6		LVGQSIIAYLQK
α-COP	620	LVGQSIIAYLQK 631
Peptide 7		LSFLYLITGNLEK
α-COP	703	VSFLYLITGNLEK 715
Peptide 8		EYIVGLSMEIDR
α-COP	1059	EYIVGLSVETER 1070
Peptide 9		TAVNLFFK
α-COP	1107	TALNLFFK 1114
Peptide 10		VTTVTEIGKDVIGLR
α-COP	1203	VTTVTEIGKDVIGLR 121

(b)

Peptide 1		VLSTPDLEVR
β-COP	328	VLSTPDLEVR 337
Peptide 2		ESGELKPEDDVTVGPAQK
β-COP	496	EAGELKPEEEITVGPVQK 513
Peptide 1		VFNYNTLER
β'-COP	83	VFNYNTLER 91
Peptide 2		HSEIQQANLK
β'-COP	319	HSEVQQANLK 328
Peptide 3		LPEAAFLAR
β'-COP	751	LPEAAFLAR 759
Peptide 4		TYLPSQVSR
β'-COP	760	TYLPSQVSR 768

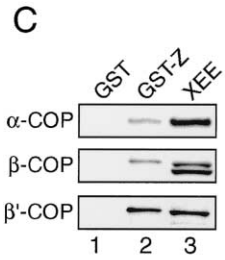

Figure 3. The Zinc Finger Domain of Nup153 Associates with the COPI Complex

(A) Silver staining of gel from a GST pull-down assay. 2% of input (XEE, *Xenopus* egg extract) was loaded in lane 1. Proteins recovered with beads coated with GST and the GST-zinc finger domain fusion are in lanes 2 and 3, respectively. Molecular markers indicated are 198, 115, and 93 kDa. "(a)" and "(b)" indicate two bands subjected to peptide sequencing.

(B) Sequences of peptides obtained from band (a) and band (b). All sequences are aligned with those of homologous human proteins in the database.

(C) Immunoblot of GST pull-down samples. Material bound to GST beads (lane 1) or GST-Z beads (lane 2) was probed with antibodies against human α-COP, β-COP, and β′-COP. Two percent of the input was loaded in lane 3.

of these antibodies to the nuclear disassembly assay prevented nuclear envelope breakdown (86% nuclei remaining at the mitotic time point; Figure 4C, panel f). This protective effect was blocked by inclusion of the immunogenic peptide (Figure 4C, panel j) and was not observed with antibodies isolated from preimmune sera (Figure 4C, panel d). This leads us to conclude that β-coatomer, and likely the entire COPI complex, plays a critical role in disassembly of the nuclear envelope.

COPI Recruitment to Nuclear Membranes Is Facilitated by Nup153 and Dependent on ARF

Our findings predict that COPI is recruited to the nuclear envelope at an early stage of mitosis. Indeed, the Golgi machinery is known to disperse around the nuclear periphery during prophase (see Shorter and Warren, 2002, and references within); however, to our knowledge the dynamic distribution of the Golgi has not been followed in relation to markers of the nuclear envelope or nuclear pores themselves. To investigate the localization of β-coatomer at different stages of the cell cycle, we first probed for its localization in conjunction with that of cyclin B in HeLa cells. Indirect immunofluorescence of cells in interphase reveals cyclin B in a diffuse staining pattern and β-coatomer predominantly in a pattern distinctive of the Golgi apparatus, clustered intensely at one side of the nucleus (Figure 5A, panels a and b). In cells at early prophase, as determined by the appearance of cyclin B in the nucleus, dramatic reorganization of the Golgi apparatus is clear, with β-COP found in a rim around the nucleus (Figure 5A, panels a and b, cells indicated by arrows). To determine whether this localization of coatomer coincides with the nuclear envelope, we simultaneously visualized β-COP and FG-rich nucleoporins. This analysis revealed a close juxtaposition of β-COP and nucleoporins (Figure 5B, cells indicated by arrows). This observation is further underscored using confocal microscopy, where there is a clear distinction between the position of the Golgi relative to the nucleus at interphase (Figure 5C, panel a) and the more intimate proximity seen as the Golgi disperses around the nucleus (Figure 5C, panel b).

To further probe the connection between the population of COPI that colocalizes with the nuclear envelope

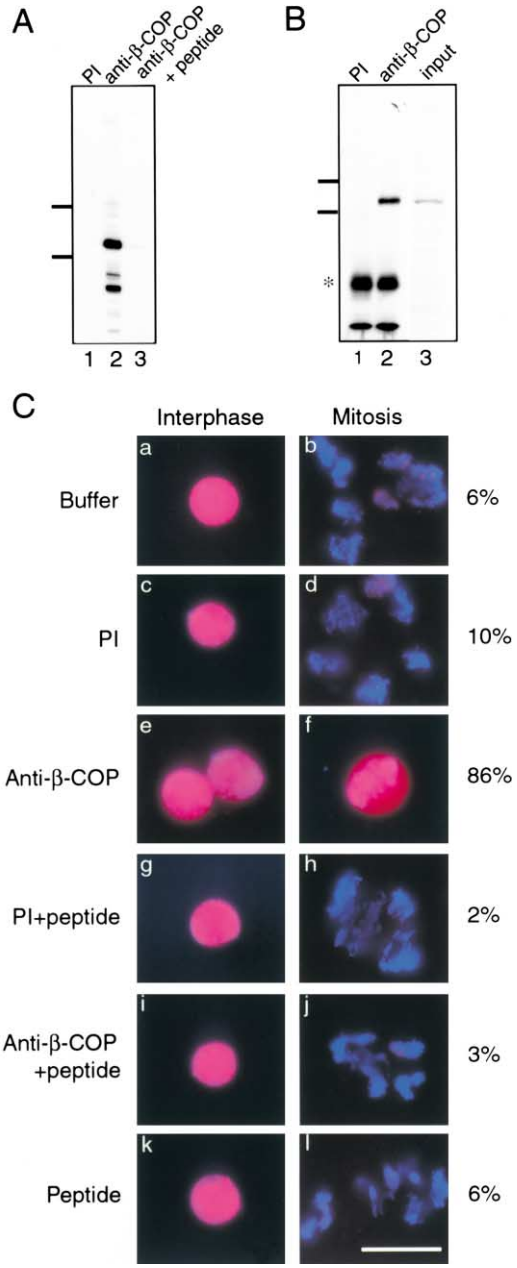

Figure 4. Anti-β-COP Inhibits Nuclear Envelope Breakdown

(A) Immunoblot of egg extract probed with preimmune (lane 1) and anti-*Xenopus*-β-COP peptide antibody (lane 2). In lane 3, anti-β-COP (0.2 μg/ml) was incubated with β-COP peptide (0.2 μg/ml) for 15 min at room temperature before adding to the blot. In both (A) and (B), molecular weight markers indicated are 115 and 93 kDa.

(B) Immunoprecipitation of egg extract with preimmune antibody (lane 1) and anti-*Xenopus* β-COP peptide antibody (lane 2). In lane 3, 2% of input egg extract was loaded. The blot was probed with anti-*Xenopus*-β-COP peptide antibody. The asterisk indicates IgG.

(C) Buffer (ELB), antibodies (5 μg), and β-COP peptide (5 μg) were added 15 min prior to the assembly/disassembly assay. In "PI + peptide" and "anti-β-COP + peptide," antibodies were incubated with the peptide for 15 min at room temperature before adding to crude egg extract. Samples were processed as described in Figure 1. Merged images of nuclear import cargo (red) and DNA (blue) are shown; the bar in panel l indicates 50 μm.

and the process of nuclear envelope breakdown, we next used nuclei assembled in the *Xenopus* egg extract. First, we examined the kinetic relationship between the appearance of β-COP at the nuclear rim and nuclear envelope breakdown. Before cyclin is added, some β-coatomer is seen by indirect immunofluorescence, likely due to its presence on membranes associated superficially with the nuclei (Figure 5D, panel a). Under these same conditions, an antibody directed against nuclear pore proteins (mAb414) clearly decorates the nuclear rim (Figure 5D, panel e). Forty minutes after triggering mitotic signals by cyclin addition, a rim stain similar to that seen for nucleoporins was detected with antibodies directed against β-coatomer (Figure 5D, panels c and g). This localization persisted at 60 min (Figure 5D, panel d), immediately prior to nuclear envelope breakdown. The specificity of this detection was confirmed by blocking reactivity of the antibodies with the immunogenic peptide (data not shown). To look at the role that Nup153 plays with respect to COPI, we next examined whether the zinc finger region of Nup153 alters the localization pattern of COPI at the nuclear envelope. Nuclei were assembled in the presence of GST or GST-Z, and the reactions were shifted to mitotic conditions by the addition of cyclin. Samples that contained the zinc finger domain, and hence held at a stage prior to nuclear envelope breakdown, showed reduced recruitment of β-coatomer to the nuclear envelope 60 min post cyclin addition (Figure 5E, compare panels e and f to panels a and b). In these same samples, normal levels of mAb414-reactive nucleoporins were observed at the nuclear rim (Figure 5E compare panels g and h to panels c and d). Thus, this region of Nup153 likely exerts a dominant-negative effect on nuclear envelope breakdown by reducing recruitment of the COPI complex.

As a further test of the proposed role for COPI in nuclear envelope breakdown, we used a peptide, derived from the small GTPase ARF1 (amino acids 2–17), that has previously been shown to interfere with ARF1-dependent coatomer recruitment (Kahn et al., 1992). Nuclear assembly proceeded in the presence of this peptide; continuous nuclear envelopes with functional pores were observed (Figure 6A, panel c). In contrast, inclusion of the ARF peptide clearly influenced nuclear envelope breakdown, with 90% of the nuclei remaining intact 75 min after cyclin addition (Figure 6A, panel d). Nuclei in this particular reaction were found to have blebbing of the nuclear envelope, which has been found to correlate with robust nuclear formation activity (Powers et al., 1995). A control peptide, composed of the reverse sequence, had no significant effect on nuclear disassembly (Figure 6A, panel f). These results indicate that efficient nuclear envelope breakdown requires the participation of ARF. This conclusion is further corroborated by our finding that Brefeldin A, a small molecule that inhibits the exchange factor for ARF, interferes with nuclear envelope breakdown (Figure 6B, panel d). Thus, the machinery involved in COPI recruitment to the nuclear membrane likely consists of a prototypic member of the well-characterized coat forming cycle, ARF, as well as an unexpected modulator of this process, Nup153.

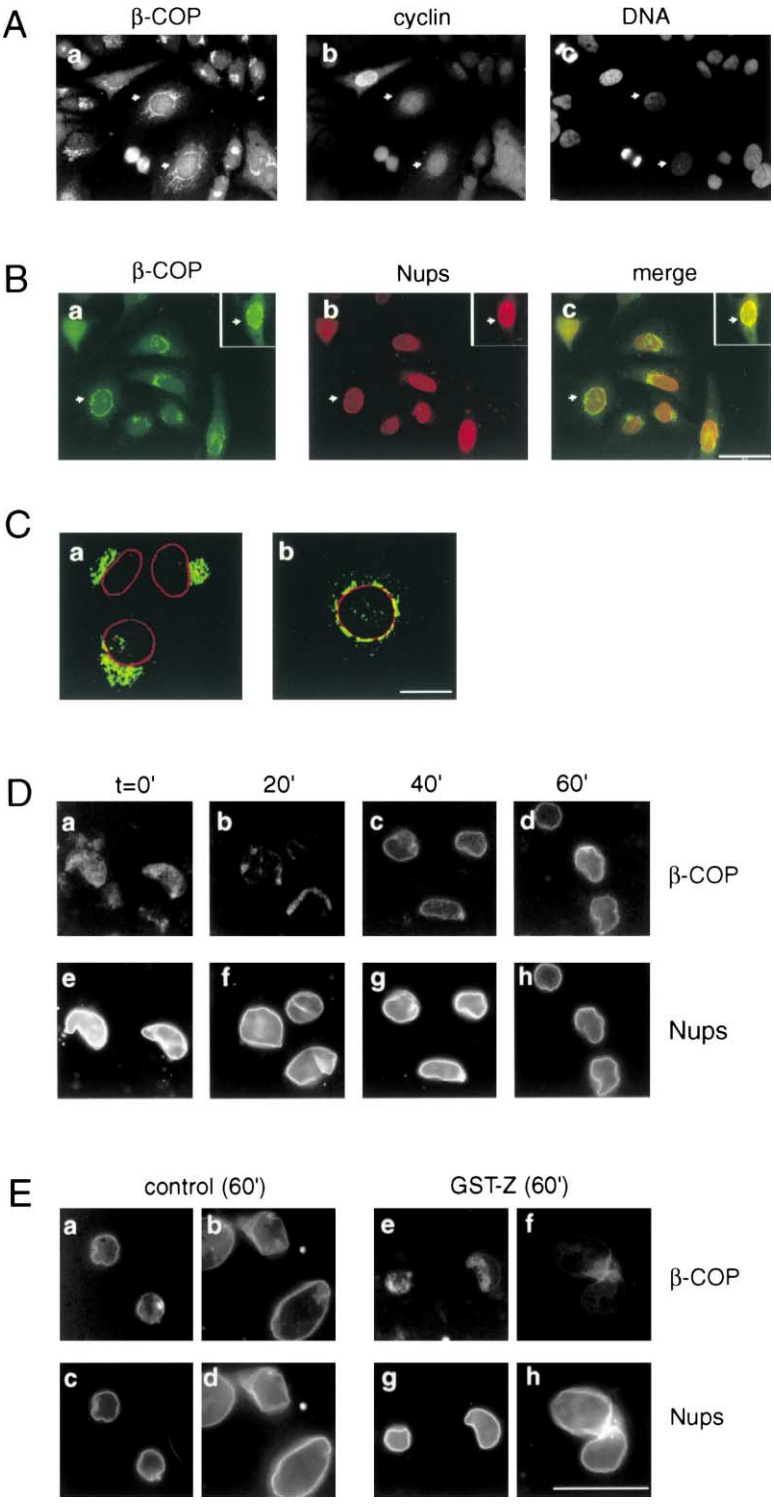

Figure 5. β-COP Is Recruited to the Nuclear Envelope during Nuclear Disassembly

(A) Indirect immunofluorescence was performed on HeLa cells following cell cycle synchronization. Cells in early prophase (indicated by arrows) show nuclear accumulation of cyclin B (panel b). The localization of β-COP is shown in panel a, and Hoechst detection of DNA is shown in panel c.

(B) Under the same conditions described above, both β-COP (panel a) and nuclear pore proteins reactive with mAb414 (panel b) were detected. The merge of the two images is seen in panel c, and arrows highlight cells exhibiting colocalization. The size bar in panel c indicates 50 μm for panels in both (A) and (B).

(C) HeLa cells treated as above were examined by confocal microscopy for β-COP (green) and nuclear pore proteins (mAb414, red). The size bar in panel b indicates 25 μm.

(D) Localization of mAb414-reactive nucleoporins (panels e–h) and β-COP (panels a–d) during in vitro nuclear disassembly. Time is either immediately prior to cyclin addition (panels a and e), or 20 min (panels b and f), 40 min (panels c and g), and 60 min (panels d and h) after cyclin addition.

(E) Recombinant zinc finger region (3 μg; 1.5 μM final concentration) was added 15 min prior to the assembly/disassembly assay. The same volume of buffer (ELB) was added to controls. Samples were examined 60 min after the addition of cyclin. Samples in panels a, c, e, and g are from one experiment, and panels b, d, f, and h are from an independent experiment. The bar in panel h indicates 50 μm for all panels in (D) and (E).

COPI-Mediated Recruitment to the Nuclear Envelope Influences a Specific Cell Cycle-Regulated Event

Having discovered several ways of interfering with nuclear envelope breakdown in the course of these studies, we had the opportunity to begin to probe the interconnections between mitotic events. For instance, we noted that chromosome condensation appeared to take place in samples where nuclear envelope breakdown was inhibited (for example, see Figure 4, panel f). To gain further insight into the question of how nuclear envelope breakdown is integrated with other events at this stage of the cell cycle, we examined whether nuclear lamina disassembly proceeded under conditions in

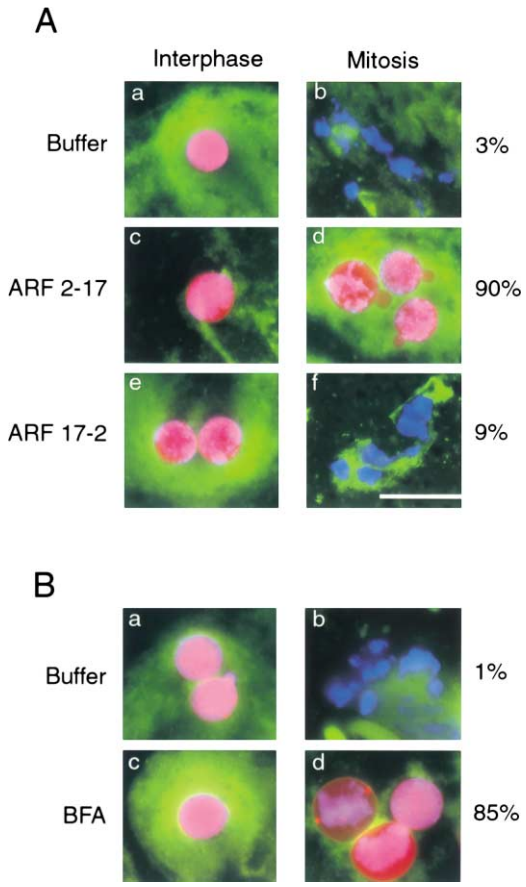

Figure 6. Inhibitors of ARF Function Interfere with Nuclear Envelope Breakdown

(A) Buffer (ELB) or ARF peptides (22 μM, final concentration) were added 15 min prior to the beginning of the assembly/disassembly assay. Samples were examined after 90 min of assembly conditions (Interphase) and 75 min after cyclin was added (Mitosis). In the merged images, DNA (Hoechst 33258) is shown in blue, NLS import substrate is shown in red, and membranes (DHCC) are shown in green. Numbers to the right of the panel indicate the percentage of intact nuclei at the 75 min postcyclin time point; the bar in panel f indicates 50 μm for all panels in (A) and (B).

(B) Buffer (ELB) or Brefeldin A (BFA) was added 15 min prior to the beginning of the assembly/disassembly assay and analyzed as described in Figure 6A.

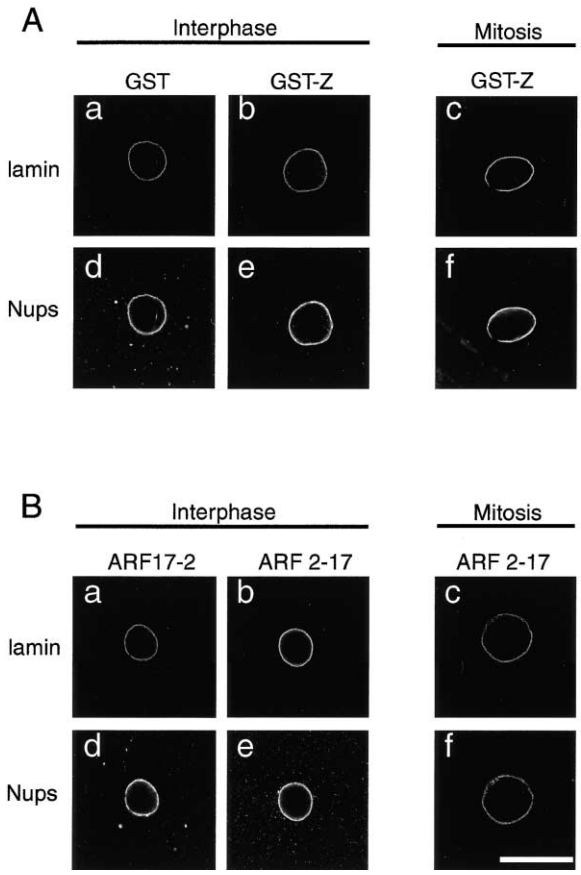

Figure 7. Prevention of Nuclear Envelope Breakdown Corresponds to a Block in Nuclear Lamina Disassembly

(A) Recombinant protein fragments (4 μg) were added to egg extract 15 min prior to the assembly/disassembly assay. The interphase samples were taken after 90 min of assembly, and the mitotic samples were taken 75 min after the addition of cyclin. Detection of the lamins is shown in panels a–c, and nuclear pore proteins reactive with mAb414 are shown in panels d–f. The samples were imaged with confocal microscopy.

(B) ARF peptides (11 μM, final concentration) were incubated 15 min prior to the assembly/disassembly assay. Samples were analyzed as described in Figure 7A. The bar in panel f indicates 50 μm for all panels in (A) and (B).

which nuclear envelope breakdown was inhibited. Indirect immunofluorescence revealed that the nuclear lamina appears intact in nuclei that persist under mitotic conditions in the presence of the Nup153 zinc finger fragment (Figure 7A, panel c). Interestingly, this was also the case when disassembly was blocked by inclusion of ARF-inhibitory peptides (Figure 7B, panel c). This suggests that a mechanism exists to couple recruitment of COPI to the nuclear envelope with disassembly of the nuclear lamina.

Discussion

Nucleoporins: Players in Nuclear Envelope Breakdown

Global changes at the nuclear pore have been shown to precede nuclear envelope breakdown (Lenart et al., 2003; Terasaki et al., 2001). Pore components have also been proposed to have a role early in prophase as anchor points at the nuclear surface for a dynein-dynactin complex, although this is still speculative (Aitchison and Rout, 2002; Beaudouin et al., 2002; Salina et al., 2002). The functional connection reported here between Nup153 and COPI illustrates another way in which a nucleoporin can contribute to nuclear disassembly. It remains possible that Nup153 plays other important roles at this step via additional mechanisms such as transport regulation. Indeed, by participating at more than one level in nuclear envelope breakdown, nucleoporins may help to coordinate different mechanisms that underlie nuclear division.

One reason that a role for Nup153 in COPI recruitment

was surprising is the localization of Nup153 predominantly on the nuclear basket structure of the nuclear pore (Pante et al., 1994; Walther et al., 2001). However, the coatomer complex may gain access to Nup153 through traditional import mechanisms or via mitosis-specific alterations in nucleocytoplasmic flux. It is also noteworthy that Nup153, although considered a component of the nuclear pore basket, is exposed on the cytoplasmic side of the pore as well (Fahrenkrog et al., 2002; Nakielny et al., 1999). The zinc finger domain itself does not appear to be accessible on the cytoplasmic face of the pore (Fahrenkrog et al., 2002), but reconfiguration of the pore early in mitosis (Lenart et al., 2003) could lead to its exposure and the opportunity for direct access with the COPI complex. Finally, large-scale perforations in the nuclear envelope, shown to occur in somatic cells at mitosis (Beaudouin et al., 2002; Salina et al., 2002), suggest that, at least after these initial events, there is ample opportunity for cytoplasmic components to access nuclear binding partners. These and other possibilities are not mutually exclusive and illustrate the range of mechanisms that could promote the partnership between Nup153 and coatomer proteins.

The specific domain of Nup153 that has been identified in this study to participate in nuclear envelope breakdown also gives rise to interesting implications. Such a zinc finger is found in one additional vertebrate pore protein, Nup358/RanBP2, raising the question of whether Nup358 also plays a role in recruitment of the COPI machinery. We are currently exploring this interesting possibility, but it is important to note that our results with two independent antibodies to Nup153 (Figure 2) indicate that, if Nup358 does participate at this step as well, it does so in a nonredundant fashion. A more distantly related zinc finger motif is found in Npl4, a protein that has been implicated in the process of nuclear assembly (Hetzer et al., 2001). Interestingly, the zinc finger of Npl4 was recently demonstrated to interact with ubiquitin (Meyer et al., 2002; Wang et al., 2003). While a zinc finger derived from Nup358 does not bind ubiquitin (Meyer et al., 2002), these studies raise the question of whether a ubiquitin-related modification is a determinant of interactions with the Nup153/Nup358 class of zinc finger. Also of note is the observation that the small GTPase Ran can interact with the zinc finger of Nup153 (Nakielny et al., 1999), suggesting that Ran, which is known to play an important role in nuclear envelope assembly, is a candidate for modulating recruitment of the COPI complex to Nup153.

Integrating Vesiculation into a Working Model of Nuclear Envelope Breakdown

Previous reports have pointed toward a thorough dispersal of integral nuclear membrane proteins into the ER (Ellenberg et al., 1997; Yang et al., 1997). Since vesicles did not appear to be an endpoint of nuclear envelope breakdown in these studies and because lateral movement between the nuclear envelope and ER membranes could explain the observed absorption of nuclear envelope into the ER, a role for vesiculation has been largely discounted (Burke and Ellenberg, 2002; Collas and Courvalin, 2000). The results here, however, suggest that vesicles formed from the nuclear envelope by a COPI-mediated pathway could in fact be an additional mechanism for dispersing the contents of the nuclear envelope into the ER via consequent fusion with the ER (see Yang et al., 1997). Indeed, electron microscopic data, in which vesicles were seen at the nuclear envelope, support this conclusion (Cotter et al., 1998). However, vesicle intermediates during nuclear envelope breakdown are not routinely observed by electron microscopy, suggesting that this contribution to nuclear envelope breakdown is rapid or spatially restricted.

Breakdown of the Golgi apparatus, like the nuclear envelope, appears to be the result of multiple mechanisms (Rossanese and Glick, 2001; Shorter and Warren, 2002). One common theme in the current views of Golgi disassembly is that COPII-mediated ER to Golgi traffic is blocked at mitosis (Featherstone et al., 1985) while COPI-mediated budding from the Golgi continues or even escalates during the initial stages of mitosis (Zaal et al., 1999). Our results point toward COPI playing an analogous role in facilitating nuclear envelope dispersal. Specifically, we have found that functionally interfering with the COPI machinery prevents nuclear disassembly (Figure 4). We also observed that during reorganization of the Golgi apparatus at mitosis, there is a stage at which the fragmented Golgi closely aligns with the nuclear envelope (Figures 5A–5C). We obtained similar results using a different marker of the Golgi (α-mannosidase) and a different cell line, BHK (data not shown), indicating that this is a general phenomenon and that the Golgi apparatus is itself closely juxtaposed with the nuclear envelope. Although, at the level of light microscopy, we cannot address whether the COPI machinery associates with the nuclear envelope in addition to Golgi membranes in intact cells, the close proximity observed is consistent with an additional role for the COPI complex at the nuclear envelope at this stage of the cell cycle. The in vitro system of nuclear assembly/disassembly gave us the opportunity to look at β-COP distribution in the absence of the Golgi. Here, we observed β-COP recruitment to the nuclear envelope during early mitosis (Figure 5D) and, moreover, found that the zinc finger fragment of Nup153 interferes with this recruitment step (Figure 5E). A role for the coatomer machinery in nuclear envelope breakdown does not preclude the notion that other mechanisms contribute to this process. Rather, this new information indicates that multiple mechanisms provide a failsafe mode of nuclear envelope breakdown, reflecting the importance of faithful segregation of the nuclear envelope and the genomic content itself.

Parallels between the Nuclear Envelope and the Golgi

Consistent with commonalities observed between Golgi and nuclear envelope disassembly, these organelle membranes also share specific aspects of biogenesis machinery. Nuclear envelope closure requires the AAA-ATPase, p97, and its partners Npl4/Ufd1 (Hetzer et al., 2001). Then, during nuclear envelope growth, p97 is again required but now in conjunction with a different partner, p47 (Hetzer et al., 2001). p97, along with p47, has been previously implicated in formation of Golgi and transitional ER following mitosis (Acharya et al., 1995; Kondo et al., 1997; Rabouille et al., 1995). This close

connection between Golgi-ER biogenesis/trafficking and nuclear envelope formation is further underscored by recent results in *S. cerevisiae*, which demonstrate altered nucleoporin distribution in mutants of several proteins involved in ER/Golgi trafficking (Ryan and Wente, 2002).

In contrast to these recently recognized corollaries, past studies focused on the role of ARF1 had led to the conclusion that this small GTPase does not have a critical role in nuclear envelope assembly or breakdown (Gant and Wilson, 1997). It seems likely that the ARF peptide used in our experiments (Figure 6A) provided a more complete block to ARF function than did size-dependent ARF depletion (Gant and Wilson, 1997). A depletion approach can be complicated by the biological activity of residual protein even at extremely low concentration. This is well illustrated by early studies of mitotic extracts in which an overall 10-fold dilution delayed complete nuclear breakdown only 2-fold (Newport and Spann, 1987). Having obtained several lines of evidence for a role of ARF and coatomer, we were prompted to reexamine the question of whether Brefeldin A affects nuclear envelope breakdown. While we saw very clear interference of nuclear envelope breakdown (Figure 6B), alternative mechanisms that contribute to this process may eventually lead to disassembly even when COPI recruitment has been compromised. Thus, an effect of Brefeldin A may be less evident as the extract progresses through mitosis and, similarly, could be masked to some extent in somatic cells, where it is clear that a combination of mechanisms leads to efficient nuclear envelope breakdown.

Cell Cycle Control of Nuclear Envelope Breakdown

This and other recent studies have highlighted that, far from being a passive process, nuclear envelope breakdown relies on a critical set of activities. Moreover, our observation that prevention of the COPI-mediated step in nuclear envelope breakdown leads to a parallel arrest in nuclear lamina breakdown (Figure 7) points toward a mechanistic link between these particular events. In previous studies, lamina solubilization was demonstrated to take place under conditions where factors necessary for nuclear envelope breakdown had been titrated to prevent disassembly of the nuclear envelope (Newport and Spann, 1987). A model consistent with these previous results, as well as with the results presented here, is that *recruitment* of COPI complexes to the nuclear pore provides a permissive signal for nuclear lamina breakdown. In the previous study, this initial recruitment step could have occurred even when factors necessary to complete nuclear envelope breakdown were limiting. In contrast, in the experiments reported here, the recruitment step itself was targeted for inhibition, consequently preventing the hypothetical permissive signal for lamina disassembly. While the molecular nature of the link between COPI recruitment and nuclear lamina breakdown is not yet elucidated, Nup153 is a good candidate for coordinating these steps since it is known to associate with both lamin (Smythe et al., 2000) and the COPI complex (this study). It will be interesting to probe this connection further as well as to investigate how the events of nuclear envelope breakdown are integrated into the intricate network of feedback that occurs during the cell cycle. For instance, the observation that dispersal of the Golgi apparatus from its pericentriolar localization is a critical control point in cell cycle progression (Sutterlin et al., 2002) may relate to a role for the coatomer machinery at the nuclear envelope. Finally, it will be important to determine how coatomer-mediated events work in concert with other mechanisms to achieve nuclear envelope breakdown in cells at different stages of development and under different proliferative states.

Experimental Procedures

Recombinant Protein Production and Purification

Recombinant protein was induced with 1 mM isopropylthio-β-D-galactoside (IPTG) for 3 hr at 37°C. Bacteria were lysed by two different methods, either in the presence of sarkosyl to promote solubilization (Frangioni and Neel, 1993) or in a PBS-based buffer with lysozyme and deoxycholate. The GST fusion proteins were purified using glutathione-Sepharose 4B resin (Amersham) according to the manufacturer's protocol. Constructs encoding amino acids 426–655 (GST-N) and 655–926 (GST-Z) were kind gifts of Sundeep Shah and Douglass Forbes. Amino acid numbers are based on conceptual translation of the *Xenopus* Nup153 N terminus (Genbank accession AF434196; Dimaano et al., 2001) combined with the original clone (Genbank accession AF045567; Shah et al., 1998).

Generation and Affinity Purification of Antibodies

The purified recombinant Nup153-N and Nup153-Z fragments were used to produce immune antisera at Zymed Laboratories. The antibodies were then affinity purified following standard procedures using a matrix with covalently coupled fragment. Preimmune antiserum was protein A purified following standard procedures. Antiserum against a synthetic internal peptide of *Xenopus* β-COP, (C)ESGELKPEDDVTVGPAQK, was also generated in rabbits at Zymed Laboratories. This peptide sequence was obtained in our mass spectrometry analysis and corresponds to amino acid residues 496–513 of human β-COP (accession #NP_057535). A cysteine residue was included at the N terminus of the peptide to allow coupling to the carrier for immunization as well as to SulfoLink sepharose (Pierce) for affinity purification.

Preparation of *Xenopus* Egg Extracts

Interphase *Xenopus* egg extracts were prepared using egg lysis buffer (ELB; 250 mM sucrose, 50 mM KCl, 2.5 mM $MgCl_2$, 10 mM HEPES [pH 7.4]) supplemented with 1 mM dithiothreitol (DTT), 5 μg/ml cytochalasin B, aprotinin and leupeptin (10 μg/ml each), and 50 μg/ml cycloheximide (Powers et al., 2001). Eggs were lysed by centrifugation for 15 min at 10,000 rpm. The cytoplasmic layer was collected as crude extract. For preparation of fractionated egg extract, the crude extract was further centrifuged for 1.5 hr at 268,000 × g. The clarified supernatant was removed and further centrifuged for 1 hr at 259,000 × g to remove residual membranes. The crude extract was stored in liquid nitrogen; fractionated extract was frozen in liquid nitrogen and then stored at −80°C.

GST Pull-Down and Identification of Associated Proteins

Fifty micrograms of GST or GST-Z was loaded onto 15 μl bead volume of preequilibrated glutathione-Sepharose for 1 hr in 300 μl of pull-down buffer (50 mM HEPES [pH 7.8], 5 mM $MgCl_2$, 200 mM NaCl, 0.5% Triton X-100, 2 μg/ml aprotinin and leupeptin), which was used throughout this procedure. After washing with 3 × 1 ml buffer, the beads were incubated with 50 μl of fractionated egg extract in a total volume of 500 μl, and the mixture was rotated for 2 hr at room temperature. The beads were then washed with 4 × 1 ml buffer and 1 × 1 ml of PBS. The bound proteins were eluted with 100 mM glycine (pH 2.5), precipitated with trichloroacetic acid and separated on 6.3% SDS-PAGE gel. Proteins were stained using the SilverQuest silver staining kit (Invitrogen). Gel bands were excised, washed with 50% acetonitrile, and stored at −80°C before sending out for peptide sequencing. Sequence analysis was performed at the Harvard Microchemistry Facility by microcapillary reverse-phase

HPLC nanoelectrospray tandem mass spectrometry (μLC/MS/MS) on a Finnigan LCQ DECA quadrupole ion trap mass spectrometer.

Immunoprecipitation and Immunoblotting

Immunoprecipitation and immunoblotting were performed following standard procedures. Antibodies used were obtained as follows: anti-GST was a kind gift of Dr. Sarah Guadagno; mAb414, which recognizes Nup62, Nup153, Nup214, and Nup358, was purchased from Covance; anti-α-COP, anti-β-COP, and anti-β′-COP were purchased from Affinity BioReagents, Inc.; goat anti-rabbit HRP and goat anti-mouse HRP were purchased from Zymed Laboratories, Inc.

In Vitro Nuclear Disassembly Assay and Microscopy

Demembranated condensed sperm chromatin was isolated from *Xenopus* testes as described previously (Powers et al., 2001). For the assembly of nuclei, an ATP-generating system was added to 28 μl of crude egg extract. Sperm chromatin was added, and nuclei were allowed to assemble by incubation at room temperature. After assembly for 1 hr, import substrate (NLS-HSA-RITC; prepared as in Powers et al., 2001) was added to the reaction and incubated for another 30 min to assess the presence of functional pores and membrane integrity. Recombinant cyclin B (Δ90; a kind gift of James Stray) with a deletion that confers stability was then added to the nuclei to initiate mitotic events (Murray et al., 1989). Samples were taken from the reaction at the indicated time points to monitor by fluorescence microscopy using DHCC (Calbiochem) to monitor membranes and Hoechst 33258 (Calbiochem) to monitor DNA.

To examine the effects of protein fragments and antibodies on nuclear disassembly, the reagent in question was incubated with crude extract for 15 min at room temperature prior to the addition of sperm chromatin and energy mix. As noted, for protein fragments either 3 μg (corresponding to final concentrations of 3.3 μM, 1.7 μM, and 1.5 μM for GST, GST-N, and GST-Z, respectively) or 4 μg (corresponding to final concentrations of 4.4 μM and 2 μM for GST and GST-Z, respectively) was added. For antibody studies, 2.5 μg of antibodies against Nup153 (and corresponding preimmune antibodies) and 5 μg of anti-β-COP (or preimmune) were used. In order to assess the effect of ADP-ribosylation factor 1 (ARF1) on nuclear disassembly, an inhibitory peptide of ARF1, GNMFANLFKGLFGKKE (ARF 2-17; represents amino acid residues 2–17 of *Xenopus* ARF1, accession #AAA74582), was synthesized (Peptide Core Facility, University of Utah). Another peptide with the reverse sequence, EKKG FLGKFLNAFMNG (ARF 17-2), was synthesized in addition and used as a control. Purities of both peptides were above 95%. These peptides (at 11 or 22 μM as indicated) were also added 15 min prior to initiation of nuclear assembly. Brefeldin A (Calbiochem) was added to reactions at a final concentration of 0.6 μg/ml.

Images were acquired on a Zeiss Axioskop 2 (Carl Zeiss, Inc.) using FV12, a 12 bit monochrome digital camera, and Olympus MicroSuite software (Olympus). Magnification, exposure, and processing were identical across samples in the same experiment. For quantitation, two samples were taken for the interphase time point (immediately prior to cyclin addition) and mitotic time point (75 min after addition of cyclin). All of the intact nuclei in each sample were counted, and the average of the two samples from the second time point was divided by the average of the two samples from the first time point. This number (×100) represents the relative number of nuclei that are present after an individual sample was shifted from interphase to mitosis.

Immunofluorescence

To assess the presence of β-COP, in vitro assembled nuclei were processed for immunofluorescence as described by Macaulay and Forbes (1996). Secondary antibodies used were Alexa Fluoro 488 goat anti-mouse IgG and Alexa Fluoro 568 goat anti-rabbit IgG (Molecular Probes). Images were acquired as described above. To assess the status of the nuclear lamina, aliquots of the assembly/disassembly reaction were placed between siliconized coverslips and a slide. The slides were inserted into liquid nitrogen until bubbling ceased, and the coverslips were immediately removed. The frozen samples were then fixed and dehydrated in methanol for 1 hr at room temperature. Following the blocking and antibody incubation steps, the samples were mounted in 50% glycerol containing 2 mg/ml phenylenediamine and imaged using an Olympus FVX IX70 confocal microscope.

HeLa cells plated on coverslips were synchronized by incubating in media containing 2 mM thymidine (Sigma). After 12 hr, the thymidine was washed out, and 11 hr later the samples were processed for indirect immunofluorescence microscopy as previously described (Griffis et al., 2002). This time point was chosen by monitoring cells under these conditions for progression into mitosis and selecting a time at which the culture was enriched for cells in prophase. Antibodies were as follows: anti-cyclin B1 monoclonal antibody at 1:500 (BD Biosciences), mAb414 at 1:2000 (Covance), and anti-β-COP at 1:1000 (Affinity BioRegents). Secondary antibodies and microscopy were as described above.

Acknowledgments

We would like to thank members of the Ullman lab for helpful discussion and Meda Higa and Brian Bennion for reagents. We are grateful to Dale Shumaker and Robert Goldman for the kind of gift of anti-lamin antibodies and to Chris Rodesch for sharing his expertise in microscopy. We also thank Janet Shaw, Jerry Kaplan, and Maureen Powers for critical reading of the manuscript. This work was supported by National Institutes of Health Grant GM61275 and a Burroughs Wellcome Career Award in Biomedical Science (to K.S.U.). A.J.P. was supported by a predoctoral fellowship from the National Science Foundation. We also gratefully acknowledge support from the Huntsman Cancer Foundation. Core facilities used in this study are partially supported by National Institutes of Health grant (P30 CA42014) to the University of Utah.

Received: October 15, 2002
Revised: June 13, 2003
Accepted: June 20, 2003
Published: September 8, 2003

References

Acharya, U., Jacobs, R., Peters, J.M., Watson, N., Farquhar, M.G., and Malhotra, V. (1995). The formation of Golgi stacks from vesiculated Golgi membranes requires two distinct fusion events. Cell *82*, 895–904.

Aitchison, J.D., and Rout, M.P. (2002). A tense time for the nuclear envelope. Cell *108*, 301–304.

Beaudouin, J., Gerlich, D., Daigle, N., Eils, R., and Ellenberg, J. (2002). Nuclear envelope breakdown proceeds by microtubule-induced tearing of the lamina. Cell *108*, 83–96.

Buendia, B., and Courvalin, J.C. (1997). Domain-specific disassembly and reassembly of nuclear membranes during mitosis. Exp. Cell Res. *230*, 133–144.

Burke, B., and Ellenberg, J. (2002). Remodelling the walls of the nucleus. Nat. Rev. Mol. Cell Biol. *3*, 487–497.

Collas, I., and Courvalin, J.C. (2000). Sorting nuclear membrane proteins at mitosis. Trends Cell Biol. *10*, 5–8.

Cotter, L.A., Goldberg, M.W., and Allen, T.D. (1998). Nuclear pore complex disassembly and nuclear envelope breakdown during mitosis may occur by both nuclear envelope vesicularisation and dispersion throughout the endoplasmic reticulum. Scanning *20*, 250–251.

Daigle, N., Beaudouin, J., Hartnell, L., Imreh, G., Hallberg, E., Lippincott-Schwartz, J., and Ellenberg, J. (2001). Nuclear pore complexes form immobile networks and have a very low turnover in live mammalian cells. J. Cell Biol. *154*, 71–84.

Dimaano, C., Ball, J.R., Prunuske, A.J., and Ullman, K.S. (2001). RNA association defines a functionally conserved domain in the nuclear pore protein Nup153. J. Biol. Chem. *276*, 45349–45357.

Drummond, S., Ferrigno, P., Lyon, C., Murphy, J., Goldberg, M., Allen, T., Smythe, C., and Hutchison, C.J. (1999). Temporal differences in the appearance of NEP-B78 and an LBR-like protein during Xenopus nuclear envelope reassembly reflect the ordered recruitment of functionally discrete vesicle types. J. Cell Biol. *144*, 225–240.

Ellenberg, J., Siggia, E.D., Moreira, J.E., Smith, C.L., Presley, J.F., Worman, H.J., and Lippincott-Schwartz, J. (1997). Nuclear membrane dynamics and reassembly in living cells: targeting of an inner nuclear membrane protein in interphase and mitosis. J. Cell Biol. *138*, 1193–1206.

Ewald, A., Hofbauer, S., Dabauvalle, M.C., and Lourim, D. (1997). Preassembly of annulate lamellae in egg extracts inhibits nuclear pore complex formation, but not nuclear membrane assembly. Eur. J. Cell Biol. *73*, 259–269.

Fahrenkrog, B., Maco, B., Fager, A.M., Koser, J., Sauder, U., Ullman, K.S., and Aebi, U. (2002). Domain-specific antibodies reveal multiple-site topology of Nup153 within the nuclear pore complex. J. Struct. Biol. *140*, 254–267.

Featherstone, C., Griffiths, G., and Warren, G. (1985). Newly synthesized G protein of vesicular stomatitis virus is not transported to the Golgi complex in mitotic cells. J. Cell Biol. *101*, 2036–2046.

Frangioni, J.V., and Neel, B.G. (1993). Solubilization and purification of enzymatically active glutathione S-transferase (pGEX) fusion proteins. Anal. Biochem. *210*, 179–187.

Gant, T.M., and Wilson, K.L. (1997). ARF is not required for nuclear vesicle fusion or mitotic membrane disassembly in vitro: evidence for a non-ARF GTPase in fusion. Eur. J. Cell Biol. *74*, 10–19.

Gonczy, P. (2002). Nuclear envelope: torn apart at mitosis. Curr. Biol. *12*, R242–R244.

Griffis, E.R., Altan, N., Lippincott-Schwartz, J., and Powers, M.A. (2002). Nup98 is a mobile nucleoporin with transcription-dependent dynamics. Mol. Biol. Cell *13*, 1282–1297.

Hang, J., and Dasso, M. (2002). Association of the human SUMO-1 protease SENP2 with the nuclear pore. J. Biol. Chem. *277*, 19961–19966.

Hetzer, M., Meyer, H.H., Walther, T.C., Bilbao-Cortes, D., Warren, G., and Mattaj, I.W. (2001). Distinct AAA-ATPase p97 complexes function in discrete steps of nuclear assembly. Nat. Cell Biol. *3*, 1086–1091.

Kahn, R.A., Randazzo, P., Serafini, T., Weiss, O., Rulka, C., Clark, J., Amherdt, M., Roller, P., Orci, L., and Rothman, J.E. (1992). The amino terminus of ADP-ribosylation factor (ARF) is a critical determinant of ARF activities and is a potent and specific inhibitor of protein transport. J. Biol. Chem. *267*, 13039–13046.

Kondo, H., Rabouille, C., Newman, R., Levine, T.P., Pappin, D., Freemont, P., and Warren, G. (1997). p47 is a cofactor for p97-mediated membrane fusion. Nature *388*, 75–78.

Lenart, P., and Ellenberg, J. (2003). Nuclear envelope dynamics in oocytes: from germinal vesicle breakdown to mitosis. Curr. Opin. Cell Biol. *15*, 88–95.

Lenart, P., Rabut, G., Daigle, N., Hand, A.R., Terasaki, M., and Ellenberg, J. (2003). Nuclear envelope breakdown in starfish oocytes proceeds by partial NPC disassembly followed by a rapidly spreading fenestration of nuclear membranes. J. Cell Biol. *160*, 1055–1068.

Macaulay, C., and Forbes, D.J. (1996). Assembly of the nuclear pore: biochemically distinct steps revealed with NEM, GTP gamma S and BAPTA. J. Cell Biol. *132*, 5–20.

Meyer, H.H., Wang, Y., and Warren, G. (2002). Direct binding of ubiquitin conjugates by the mammalian p97 adaptor complexes, p47 and Ufd1-Npl4. EMBO J. *21*, 5645–5652.

Moroianu, J., Blobel, G., and Radu, A. (1997). RanGTP-mediated nuclear export of karyopherin alpha involves its interaction with the nucleoporin Nup153. Proc. Natl. Acad. Sci. USA *94*, 9699–9704.

Murray, A.W., Solomon, M.J., and Kirschner, M.W. (1989). The role of cyclin synthesis and degradation in the control of maturation promoting factor activity. Nature *339*, 280–286.

Nakielny, S., Shaikh, S., Burke, B., and Dreyfuss, G. (1999). Nup153 is an M9-containing mobile nucleoporin with a novel Ran-binding domain. EMBO J. *18*, 1982–1995.

Newport, J., and Spann, T. (1987). Disassembly of the nucleus in mitotic extracts: membrane vesicularization, lamin disassembly, and chromosome condensation are independent processes. Cell *48*, 219–230.

Nickel, W., Brugger, B., and Wieland, F.T. (2002). Vesicular transport: the core machinery of COPI recruitment and budding. J. Cell Sci. *115*, 3235–3240.

Pante, N., Bastos, R., McMorrow, I., Burke, B., and Aebi, U. (1994). Interactions and three-dimensional localization of a group of nuclear pore complex proteins. J. Cell Biol. *126*, 603–617.

Powers, M.A., Macaulay, C., Masiarz, F.R., and Forbes, D.J. (1995). Reconstituted nuclei depleted of a vertebrate GLFG nuclear pore protein, p97, import but are defective in nuclear growth and replication. J. Cell Biol. *128*, 721–736.

Powers, M.A., Evans, E.K., Yang, J., and Kornbluth, S. (2001). Preparation and use of interphase *Xenopus* egg extracts. In Current Protocols in Cell Biology, J.S. Bonifacino, M. Dasso, J.B. Harford, J. Lippincott-Schwartz, and K.M. Yamada, eds. (New York: John Wiley & Sons), pp. 11.10.11–11.11.24.

Rabouille, C., Levine, T.P., Peters, J.M., and Warren, G. (1995). An NSF-like ATPase, p97, and NSF mediate cisternal regrowth from mitotic Golgi fragments. Cell *82*, 905–914.

Rossanese, O.W., and Glick, B.S. (2001). Deconstructing Golgi inheritance. Traffic *2*, 589–596.

Ryan, K.J., and Wente, S.R. (2002). Isolation and characterization of new Saccharomyces cerevisiae mutants perturbed in nuclear pore complex assembly. BMC Genet. *3*, 17.

Salina, D., Bodoor, K., Eckley, D.M., Schroer, T.A., Rattner, J.B., and Burke, B. (2002). Cytoplasmic dynein as a facilitator of nuclear envelope breakdown. Cell *108*, 97–107.

Sasagawa, S., Yamamoto, A., Ichimura, T., Omata, S., and Horigome, T. (1999). In vitro nuclear assembly with affinity-purified nuclear envelope precursor vesicle fractions, PV1 and PV2. Eur. J. Cell Biol. *78*, 593–600.

Shah, S., and Forbes, D.J. (1998). Separate nuclear import pathways converge on the nucleoporin Nup153 and can be dissected with dominant-negative inhibitors. Curr. Biol. *8*, 1376–1386.

Shah, S., Tugendreich, S., and Forbes, D. (1998). Major binding sites for the nuclear import receptor are the internal nucleoporin Nup153 and the adjacent nuclear filament protein Tpr. J. Cell Biol. *141*, 31–49.

Smythe, C., Jenkins, H.E., and Hutchison, C.J. (2000). Incorporation of the nuclear pore basket protein nup153 into nuclear pore structures is dependent upon lamina assembly: evidence from cell-free extracts of Xenopus eggs. EMBO J. *19*, 3918–3931.

Sukegawa, J., and Blobel, G. (1993). A nuclear pore complex protein that contains zinc finger motifs, binds DNA, and faces the nucleoplasm. Cell *72*, 29–38.

Suntharalingam, M., and Wente, S.R. (2003). Peering through the pore. Nuclear pore complex structure, assembly, and function. Dev. Cell *4*, 775–789.

Sutterlin, C., Hsu, P., Mallabiabarrena, A., and Malhotra, V. (2002). Fragmentation and dispersal of the pericentriolar Golgi complex is required for entry into mitosis in mammalian cells. Cell *109*, 359–369.

Terasaki, M., Campagnola, P., Rolls, M.M., Stein, P.A., Ellenberg, J., Hinkle, B., and Slepchenko, B. (2001). A new model for nuclear envelope breakdown. Mol. Biol. Cell *12*, 503–510.

Ullman, K.S., Shah, S., Powers, M.A., and Forbes, D.J. (1999). The nucleoporin nup153 plays a critical role in multiple types of nuclear export. Mol. Biol. Cell *10*, 649–664.

Vasu, S.K., and Forbes, D.J. (2001). Nuclear pores and nuclear assembly. Curr. Opin. Cell Biol. *13*, 363–375.

Vasu, S., Shah, S., Orjalo, A., Park, M., Fischer, W.H., and Forbes, D.J. (2001). Novel vertebrate nucleoporins Nup133 and Nup160 play a role in mRNA export. J. Cell Biol. *155*, 339–354.

Vigers, G.P., and Lohka, M.J. (1991). A distinct vesicle population targets membranes and pore complexes to the nuclear envelope in Xenopus eggs. J. Cell Biol. *112*, 545–556.

Walther, T.C., Fornerod, M., Pickersgill, H., Goldberg, M., Allen, T.D., and Mattaj, I.W. (2001). The nucleoporin Nup153 is required for nuclear pore basket formation, nuclear pore complex anchoring and import of a subset of nuclear proteins. EMBO J. *20*, 5703–5714.

Wang, B., Alam, S.L., Meyer, H.H., Payne, M., Stemmler, T.L., Davis, D.R., and Sundquist, W.I. (2003). Structure and ubiquitin interactions

of the conserved NZF domain of Npl4. J. Biol. Chem. *278*, 20225–20234.

Shorter, J., and Warren, G. (2002). Golgi architecture and inheritance. Annu. Rev. Cell Dev. Biol. *18*, 379–420.

Yang, L., Guan, T., and Gerace, L. (1997). Integral membrane proteins of the nuclear envelope are dispersed throughout the endoplasmic reticulum during mitosis. J. Cell Biol. *137*, 1199–1210.

Zaal, K.J., Smith, C.L., Polishchuk, R.S., Altan, N., Cole, N.B., Ellenberg, J., Hirschberg, K., Presley, J.F., Roberts, T.H., Siggia, E., et al. (1999). Golgi membranes are absorbed into and reemerge from the ER during mitosis. Cell *99*, 589–601.

Zhang, H., Saitoh, H., and Matunis, M.J. (2002). Enzymes of the SUMO modification pathway localize to filaments of the nuclear pore complex. Mol. Cell. Biol. *22*, 6498–6508.